

Water-locking molecule-assisted fabrication of natural-inspired Mg(OH)₂ for high-efficient and economical uranium capture

Hengbin Xu,^a Zhenyuan Bai,^a Milin Zhang,^{a,b,*} Jun Wang,^a Yongde Yan,^a Min Qiu^b,
Jiaming Chen^b

^aKey Laboratory of Superlight Materials and Surface Technology, Ministry of Education, College of Materials Science and Chemical Engineering, Harbin Engineering University, Harbin 150001, China

^bCollege of Science, Heihe University, Heihe 164300, China

Corresponding author: Milin Zhang

Telephone: +86-451-82569890

E-mail address: zhangmilin@hrbeu.edu.cn

S2 Experimental

S2.1 Preparation of CMC-PAM/Mg(OH)₂

Table S1 Chemical compositions of magnesite before and after calcination.

Component (%, w/w)	MgO	MgCO ₃	Mg(OH) ₂	CaO	SiO ₂	Fe ₂ O ₃	Al ₂ O ₃	MnO	Others
Original magnesite	15.36	72.63	1.25	4.25	5.57	0.77	0.13	0.03	<0.01
Calcined magnesite	6.54	5.25	78.97	3.18	5.46	0.45	0.11	0.03	<0.01

S2.2 Measurements

The specific functional groups on the CMC-PAM/Mg(OH)₂ adsorbents were detected using FT-IR spectroscopy (Avatar 370) by mixing with KBr powder. The crystallinity of samples were obtained by XRD, which performed using a RigakuD/Max-IIIB diffractometer with Cu-K α irradiation ($K\alpha = 1.54178 \text{ \AA}$). SEM (JEOL JSM-6480A, Japan Electronics) was used to observe the inner structure morphologies of the CMC-PAM/Mg(OH)₂ adsorbent. The surface chemistry of adsorbents before and after adsorption process were determined by XPS (ESCALAB 250Xi). The BET surface areas were obtained from nitrogen adsorption isotherms using an AUTOSORB-IQ2-MP analyzer.

S2.3 Methods of uranium extraction

S2.3.1 Batch adsorption in laboratory

In the adsorption experiment, the pH levels of the solutions were adjusted by 0.5

mol L⁻¹ HNO₃ or 0.5 mol L⁻¹ Na₂CO₃ aqueous solution. The solutions with different uranium concentrations were obtained by diluting the stock metal solution with the proper amount of distilled water. The high concentrations of uranium were detected by ICP-AES and low concentrations (~1 µg L⁻¹) were detected by ICP-MS. UO₂·(NO₃)₂·6H₂O (2.11 g) was dissolved in 1 L deionized water, giving a uranium concentration of 1000 mg L⁻¹ (stock metal solution). Typically, 0.02 g of adsorbent was shaken with 0.05 L uranium solution of a given pH value and concentration in a constant temperature oscillator. During this process, we changed the different experimental parameters, including the solution pH, solution concentration, adsorption time and temperature. CMC-PAM/Mg(OH)₂ adsorbents and the uranium solution were isolated by centrifugation after the adsorption processes. The adsorption capacity (Q_e) and the removal rate (R) was calculated according to the following formula:

$$Q_e = (C_0 - C_e)V/m \quad \text{eq (S1)}$$

$$R = C_0 - C_e/C_0 \times 100\% \quad \text{eq (S2)}$$

where Q_e is the adsorption capacity of the adsorbent, C_0 (mg L⁻¹) is the original concentration of U(VI) ions, C_e (mg L⁻¹) is the remaining concentration of uranium, V (L) is the volume of the solution, m is the weight of the adsorbent, and R is the adsorption removal efficiency.

The selectivity test was investigated in simulated wastewater environment. Specifically, 0.02 g of CMC-PAM/Mg(OH)₂ was immersed in 0.05 L of 200 mg L⁻¹ of the uranium solution containing a mixture of other metal ions (including transition

heavy metal ions (Mn^{2+} , Fe^{3+} , Co^{2+} , Pb^{2+} , Zn^{2+}), radioactive ions (Sr^{2+} , Cs^{2+}) and lanthanides element (Ce^{3+}), each with an initial concentration of 200 mg L^{-1} . The adsorption reaction was lasted at room temperature for 3 hours, aliquots were taken from the mixture, and the adsorbents were separated by centrifugation. The residual uranium and the other coexisting metal ion concentration in the resulting solutions were analyzed by ICP-AES.

S2.3.2 Flow-through column adsorption in laboratory

To produce a highly concentrated sea salt solution, 100 kg sea salt was first dissolved in 450 L of deionized water. The as-prepared simulated seawater was drawn from a reservoir and forced through the pipeline using a pump. Then, the solution was filtered and successively sterilized by ultraviolet radiation. The CMC-PAM/ $\text{Mg}(\text{OH})_2$ adsorbent was packed in columns of 20 cm height and 5 cm diameter. To keep the adsorbent uniformly distributed along the columns, glass beads of 4 mm diameter were packed in the upper and lower ends of the columns. The pH value of the solution was controlled to 8.3 ± 0.3 by adding a specific amount of saturated Na_2CO_3 solution. Deionized water was then pumped into the pot to adjust the salinity of the simulated seawater, which was controlled by a conductivity meter. The salinity of the simulated seawater was 35 when the conductivity value reached $49000 \pm 2000 \mu\text{S}\cdot\text{cm}^{-1}$.

S3 Results and Discussion

S3.1 Characterization and Structure Analysis.

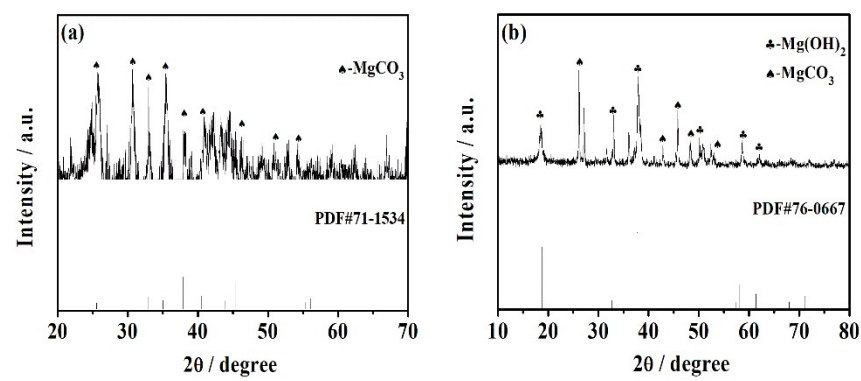


Fig. S1 XRD patterns of (a) natural magnesite, (b) $\text{Mg}(\text{OH})_2$.

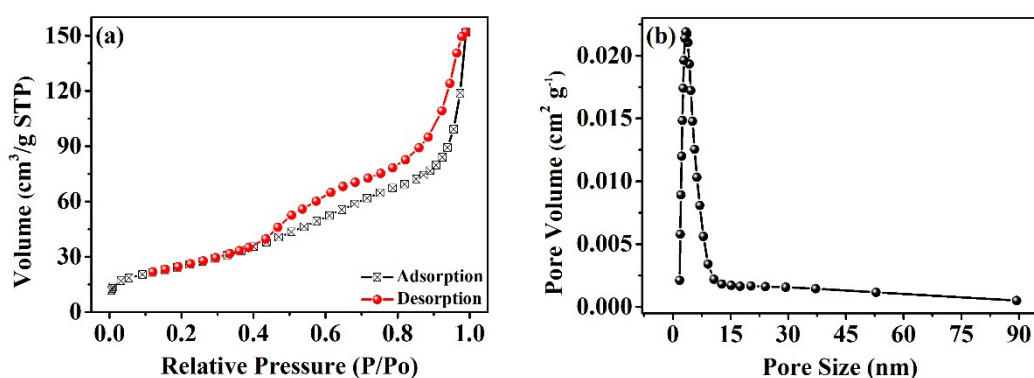


Fig. S2 (a) Nitrogen adsorption-desorption isotherms and (b) the corresponding pore size distribution of CMC-PAM/ $\text{Mg}(\text{OH})_2$.

The uranium adsorption capacity achieved the highest value with CMC:PAM: $\text{Mg}(\text{OH})_2$ ratio of 3:5:20. Therefore, in order to prepare 1 kg adsorbent with optimum ratio, the demand amount of CMC, PAM and $\text{Mg}(\text{OH})_2$ is 0.11 kg, 0.18 kg and 0.71 kg, respectively. According to the current market price, the cost of purchasing 1 ton CMC, PAM and magnesite should be RMB ¥4800-5000 (about US \$720), RMB ¥3000-3200 (about US \$440) and RMB ¥480-500 (about US \$70), respectively. Therefore, the cost per kilogram of adsorbent is estimated to be approximately US \$0.21 under the ratio of CMC:PAM: $\text{Mg}(\text{OH})_2=3:5:20$. In addition, we further evaluated the cost of field adsorption tests in natural seawater and river.

Specifically, the real-world application can be implemented in three steps, namely, preparation samples for field adsorption, the transport process and field adsorption tests. The cost of processing the powder-like CMC-PAM/Mg(OH)₂ into a form that can be used in actual field adsorption tests (put it into the cloth bag) was estimated to US \$ 3/kg. The cost of transporting the prepared samples to the field adsorption platform was about \$ 2/kg. The cost produced during the field adsorption test, including the deployment, removal and desorption of adsorbent, was approximately \$ 5/kg (Fig. S3). The adsorbent exhibited a saturation time of 27 days in Dachangshan island and reached a uranium adsorption capacity of 8.6 mg/g (Fig. 10(a)). Therefore, the needed cost for extracting 1 kg uranium should be \$1184.36. Note that though the uncertainty associated with this estimate remains considerable and future experimental data are needed to further reduce sources of uncertainty, the real-world marine test and estimated cost analysis suggested potential industrial value and economic performance of CMC-PAM/Mg(OH)₂ for uranium extraction from seawater.

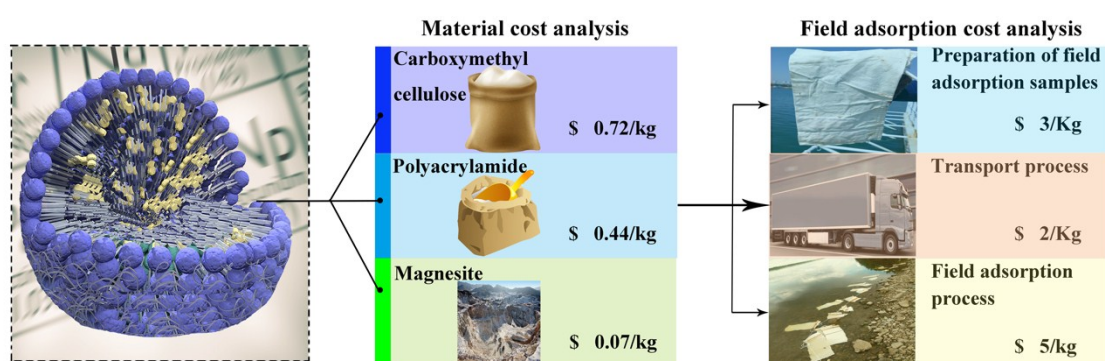


Fig. S3 The cost analysis of CMC-PAM/Mg(OH)₂ for uranium extraction.

S3.2 Adsorption experiments

S3.2.1 Effect of different proportions and pH on uranium adsorption

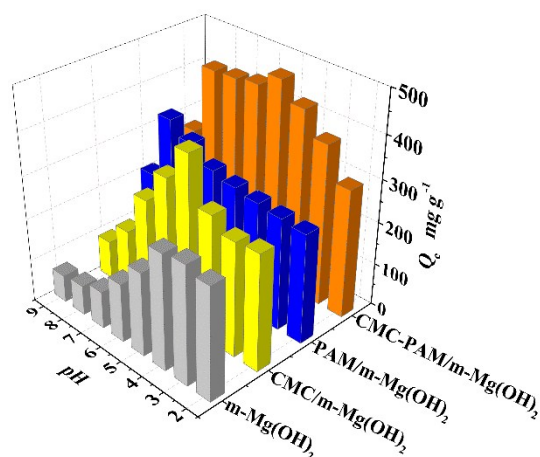


Fig. S4 Effects of pH values on the adsorption capacities of uranium on four adsorbents.

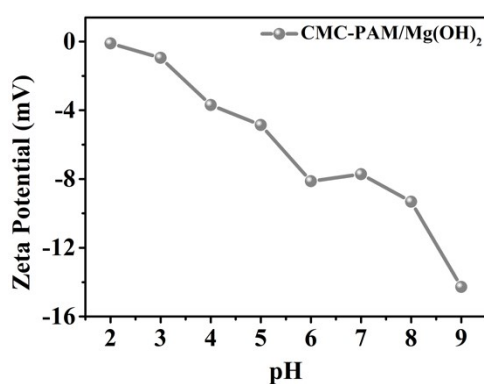


Fig. S5 Zeta-potential of CMC-PAM/Mg(OH)₂ under different pH values.

S3.2.2 Uranium Adsorption Kinetics.

The equation of pseudo-first-order model, pseudo-second order, Morris-Weber (W-M) model were illustrated as:

$$\ln(Q_e - Q_t) = \ln Q_e - k_1 t \quad \text{eq (S3)}$$

$$\frac{t}{Q_t} = \frac{1}{k_2 Q_e^2} + \frac{t}{Q_e} \quad \text{eq (S4)}$$

4)

$$Q_e = k_{ip} \sqrt{t} + C \quad \text{eq (S5)}$$

where Q_t and Q_e (mg g⁻¹) are the capacity of uranium at time t (min) and at equilibrium, k_{ip} is Internal diffusion constant, respectively, and k_1 (min⁻¹) and k_2 (g

mg⁻¹ min⁻¹) are the respective rate constants.

Table S2 The kinetic parameters for the adsorption of uranium fitting by pseudo-first-order and pseudo-second-order at pH = 5.0.

Kinetic Modes	Parameters	Adsorbent dose (mg)		
		10	20	40
Pseudo-first-order	q _e (mg g ⁻¹)	336.42	138.87	47.24
	k ₁ (L mg ⁻¹)	0.005	0.005	0.004
	R ²	0.839	0.785	0.571
Pseudo-second-order	q _e (mg g ⁻¹)	1101.31	625.00	317.46
	k ₂ (g min ⁻¹ mg ⁻¹)	3.58×10 ⁻⁵	8.72×10 ⁻⁵	1.94×10 ⁻⁴
	R ²	0.999	0.999	0.999

Table S3 The kinetic parameters for the adsorption of uranium fitting by pseudo-first-order and pseudo-second-order at pH = 8.0.

Kinetic Modes	Parameters	Adsorbent dose (mg)		
		10	20	40
Pseudo-first-order	Q _e (mg g ⁻¹)	39.20	13.38	10.22
	k ₁ (L mg ⁻¹)	0.004	0.003	0.003
	R ²	0.712	0.619	0.517
Pseudo-second-order	Q _e (mg g ⁻¹)	232.56	125.00	62.89
	k ₂ (g min ⁻¹ mg ⁻¹)	3.72×10 ⁻⁴	1.04×10 ⁻³	2.76×10 ⁻³
	R ²	0.999	0.999	0.999

S3.2.4 Uranium Adsorption Isotherms

The Langmuir, Freundlich and Dubinin-Radushkevich models were applied to simulate experimental data^{1,2}:

$$\frac{C_e}{Q_e} = \frac{1}{bQ_m} + \frac{C_e}{Q_m} \quad \text{eq (S5)}$$

$$\ln Q_e = \ln k + \frac{1}{n} \ln C_e \quad \text{eq (S6)}$$

$$\ln Q_e = \ln Q_m - \beta \varepsilon^2 \quad \text{(eq S7)}$$

where C_e (mg L⁻¹) is the equilibrated uranium concentration, Q_e (mg g⁻¹) is the amount of uranium adsorbed on the adsorbents capacity at equilibrium. b (L mg⁻¹) is a Langmuir constant related to the energy of the adsorbent and Q_m (mg g⁻¹) is the saturation capacity at complete monolayer coverage, where b is the activity coefficient and ε is the Polanyi potential. ε was calculated via the following equation

$$\varepsilon = RT \ln \left(1 + \frac{1}{C_e} \right) \quad \text{(eq S8)}$$

Table S4 Isotherm parameter for CMC-PAM/Mg(OH)₂ adsorption of uranium at pH = 5.0

Isotherm model	Parameters	T (K)		
		298.15	308.15	318.15
Langmuir	Q_m (mg g ⁻¹)	1584.67	1728.02	1902.49
	b (L mg ⁻¹)	0.07	0.08	0.09
	R^2	0.993	0.988	0.980
Freundlich	n	1.71	1.68	1.62
	k (L g ⁻¹)	116.95	138.00	168.66

	R^2	0.838	0.794	0.748
	Q_m (mg g ⁻¹)	591.04	607.97	636.57
D-R	β	0.14	0.18	0.10
	R^2	0.502	0.495	0.508

Table S5 Isotherm parameter for CMC-PAM/Mg(OH)₂ adsorption of uranium at pH = 8.0

Isotherm model	Parameters	T (K)		
		298.15	308.15	318.15
	Q_m (mg g ⁻¹)	454.55	505.05	552.49
Langmuir	b (L mg ⁻¹)	0.20	0.22	0.30
	R^2	0.997	0.997	0.996
	n	2.03	1.99	2.07
Freundlich	k (L g ⁻¹)	70.82	83.11	108.22
	R^2	0.931	0.930	0.923
	Q_m (mg g ⁻¹)	195.86	197.56	202.09
D-R	β	0.07	0.04	0.03
	R^2	0.661	0.604	0.573

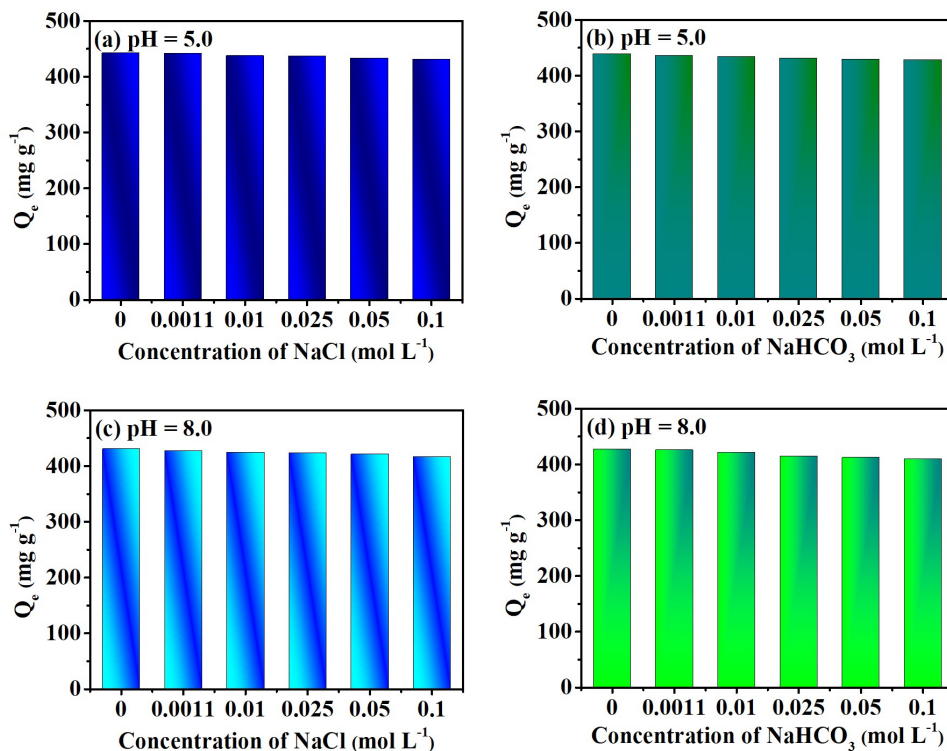


Fig. S6 Effects of NaCl ionic strength on uranium adsorption by CMC-PAM/Mg(OH)₂ at (a) pH = 5.0 and (c) pH = 8.0, Effects of NaHCO₃ ionic strength on uranium adsorption by CMC-PAM/Mg(OH)₂ at (b) pH = 5.0 and (d) pH = 8.0.

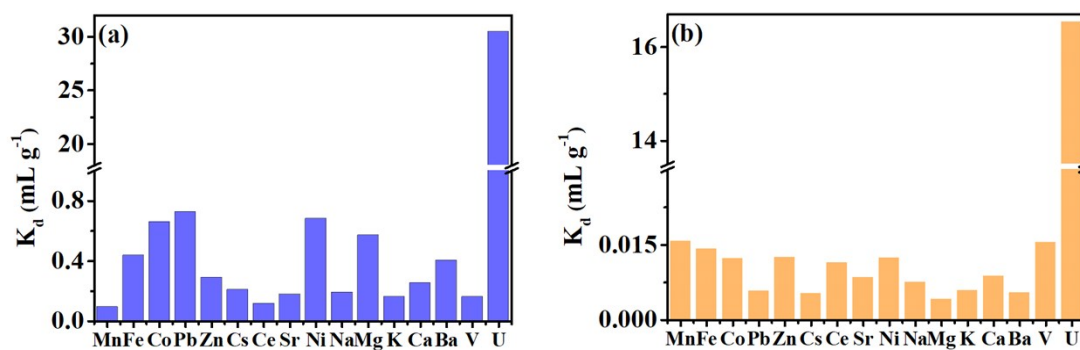


Fig. S7 K_d value of U and other interference ions in (a) deionized water containing uranium and the other ions with nearly equal concentrations ca. $1000 \mu\text{g L}^{-1}$ and (b) deionized water containing uranium ca. 1 mg L^{-1} and the other ions with nearly equal concentrations ca. 500 mg L^{-1} .

The detailed description on the method for desorption process

0.02 g CMC-PAM/Mg(OH)₂ after uranium adsorption can be regenerated by

soaking in $0.05 \text{ mol L}^{-1} \text{ Na}_2\text{CO}_3$ for 6 h in a state of shock, then the adsorbent is separated from the liquid by centrifugation and washed by deionized water three times before the next cycle adsorption experiment³.

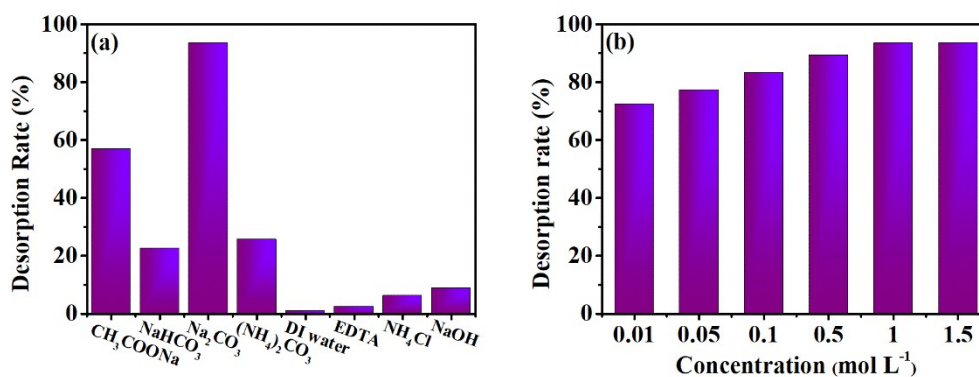


Fig. S8 Desorption efficiency of (a) different desorbent, (b) different concentration of Na_2CO_3 .

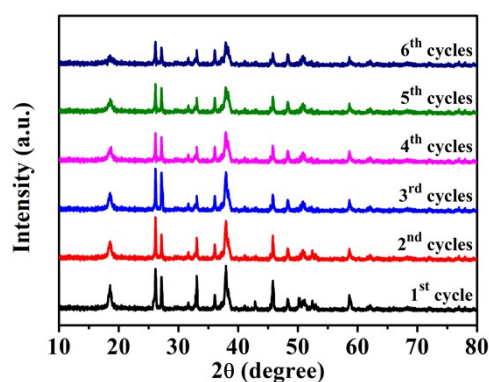


Fig. S9 The XRD pattern of CMC-PAM/Mg(OH)₂ after six cycles.

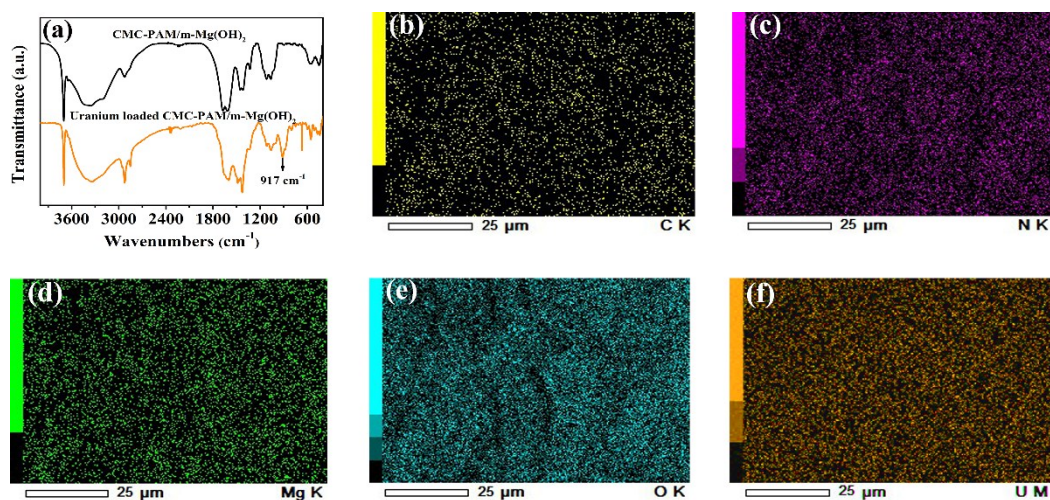


Fig. S10 (a) FTIR of CMC-PAM/Mg(OH)₂ and uranium-loaded CMC-PAM/Mg(OH)₂. The

elemental mapping of uranium-loaded CMC-PAM/Mg(OH)₂: (b) C, (c) N, (d) Mg, (e) O and (f) U

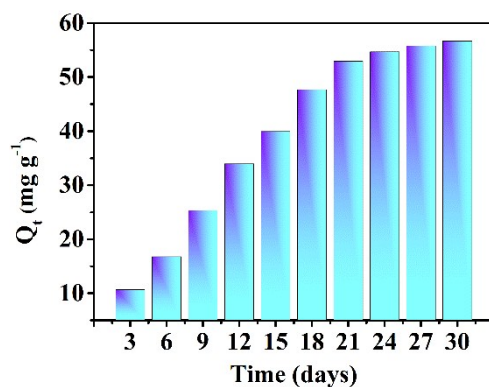


Fig. S11 The dynamic adsorption experiment with 400 L of circulated simulated seawater.

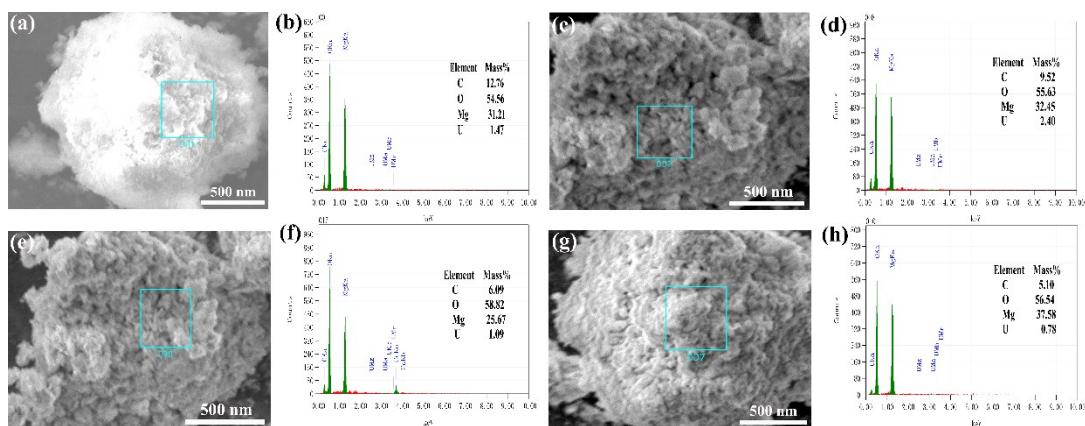


Fig. S12 The EDX of the CMC-PAM/Mg(OH)₂ immersed in the Dachangshan and Heilongjiang adsorption platform for 30 days.

Table S6 Uranium adsorption performance in natural seawater of various adsorbent materials.

Adsorbents	Adsorption capacity (mg g ⁻¹)	Adsorption time	Seawater source	Ref.	
AO-UHMWPE-1	0.25	68 days	Xiamen		
AO-UHMWPE	AO-UHMWPE-2	0.04	68 days	Xiamen	4
	AO-UHMWPE-7	1.41	15 days	Daishan	
Anti-UiO-66	4.62±0.09	30 days	Not mentioned	5	

POP-oNH ₂ -AO	4.36	56 days	Not mentioned	6
PAO hydrogel	4.87±0.38	28 days	Not mentioned	7
PIDO/Alg hydrogel	5.84±0.84	56 days	Not mentioned	8
CP-PAO composite hydrogel	6.21±0.59	42 days	Not mentioned	9
			South China sea	
UUS-1	9.46±0.39	48 h	near the boundary island	10
			South China Sea	
AO-HNTs	9.01	30 days	nearly	11
			Haikou city	
			South China sea	
SMON-PAO	9.59±0.64	56 days	near the boundary island	12
			South China sea	
PIDO NF	8.74±0.41	56 days	near the boundary island	13
	8.6±0.28	27 days	Dachangshan	
CMC-PAM/Mg(OH) ₂	6.7±0.17	18 days	Heilongjiang	This work

References

1. G. Limousin, J.P. Gaudet, L. Charlet, S. Szenknect, V. Barthes and M. Krimissa, Sorption isotherms: A review on physical bases, modeling and measurement, *Appl. Geochem.*, 2007, **22**,

249-275.

2. M. Sureshkumar, D. Das, M. Mallia and P. Gupta, Adsorption of uranium from aqueous solution using chitosan-tripolyphosphate (CTPP) beads, *J. Hazard. Mater.*, 2010, **184**, 65-72.
3. Z.J. Li, Z.W. Huang, W.L. Guo, L. Wang, L.R. Zheng, Z.F. Chai, W.Q. Shi, Enhanced Photocatalytic Removal of Uranium(VI) from Aqueous Solution by Magnetic TiO₂/Fe₃O₄ and Its Graphene Composite, *Environ. Sci. Technol.*, 2017, **51**, 5666-5674.
4. C. J. Ling, X. Y. Liu, X. J. Yang, J. T. Hu, R. Li, L. J. Pang, H. J. Ma, J. Y. Li, G. Z. Wu, S. M. Lu, D. L. Wang, Uranium Adsorption Tests of Amidoxime-Based Ultrahigh Molecular Weight Polyethylene Fibers in Simulated Seawater and Natural Coastal Marine Seawater from Different Locations, *Ind. Eng. Chem. Res.*, 2017, **56**, 1103-1111. DOI: 10.1021/acs.iecr.6b04181.
5. Q. H. Yu, Y. H. Yuan, J. Wen, X. M. Zhao, S. L. Zhao, D. Wang, C. Y. Li, Xi. L. Wang, N. Wang, A Universally Applicable Strategy for Construction of Anti-Biofouling Adsorbents for Enhanced Uranium Recovery from Seawater, *Adv. Sci.*, 2019, 1900002. DOI: 10.1002/advs.201900002.
6. Q. Sun, B. Aguila, J. Perman, A. S. Ivanov, V. S. Bryantsev, L. D. Earl, C. W. Abney, L. Wojtas, S. Q. Ma, Bio-inspired nano-traps for uranium extraction from seawater and recovery from nuclear waste, *Nat. Commun.*, 2018, **9**, 1644. DOI: 10.1038/s41467-018-04032-y.
7. C. X. Ma, J. X. Gao, D. Wang, Y. H. Yuan, J. Wen, B. J. Yan, S. L. Zhao, X. M. Zhao, Y. Sun, X. L. Wang, N. Wang, Sunlight Polymerization of Poly(amidoxime) Hydrogel Membrane for Enhanced Uranium Extraction from Seawater, *Adv. Sci.*, 2019, 1900085. DOI: 10.1002/advs.201900085.
8. D. Wang, J. N. Song, S. Lin, J. Wen, C. X. Ma, Y. H. Yuan, M. Lei, Xi. L. Wang, N. Wang, H.

Wu, A Marine-Inspired Hybrid Sponge for Highly Efficient Uranium Extraction from Seawater, *Adv. Funct. Mater.*, 2019, 1901009. DOI: 10.1002/adfm.201901009.

9. J. X. Gao, Y. H. Yuan, Q. H. Yu, B. J. Yan, Y. X. Qian, J. Wen, C. X. Ma, S. H. Jiang, X. L. Wang, N. Wang, Bio-Inspired Antibacterial Cellulose Paper-Poly(amidoxime) Composite Hydrogel for High-Efficient Uranium(VI) Capture from Seawater, *Chem. Commun.*, DOI: 10.1039/C9CC09936K.

10. Y. H. Yuan, Q. H. Yu, S. Yang, J. Wen, Z. H. Guo, X. L. Wang, N. Wang, Ultrafast Recovery of Uranium from Seawater by *Bacillus velezensis* Strain UUS-1 with Innate Anti-Biofouling Activity, *Adv. Sci.*, 2019, 1900961. DOI: 10.1002/advs.201900961.

11. S. L. Zhao, Y. H. Yuan, Q. H. Yu, B. Y. Niu, J. H. Liao, Z. H. Guo, N. Wang, Dual-surface amidoximated halloysite nanotube for high-efficient and economical uranium extraction from seawater, *Angew. Chem. Int. Edit.*, 2019, **58**, 14979-14985. DOI: 10.1002/anie.201908762

12. Y. H. Yuan, S. L. Zhao, J. Wen, D. Wang, X. W. Guo, L. L. Xu, X. L. Wang, N. Wang, Rational Design of Porous Nanofiber Adsorbent by Blow-Spinning with Ultrahigh Uranium Recovery Capacity from Seawater, *Adv. Funct. Mater.*, 2018, 1805380. DOI: 10.1002/adfm.201805380.

13. D. Wang, J. Song, J. Wen, Y. H. Yuan, Z. L. Liu, S. Lin, H. Y. Wang, H. L. Wang, S. L. Zhao, X. M. Zhao, M. H. Fang, M. Lei, B. Li, N. Wang, X. L. Wang, H. Wu, *Adv. Energy Mater.*, 2018, 1802607. DOI: 10.1002/aenm.201802607.